doi:10.1016/j.jmb.2009.03.065 J. Mol. Biol. (2009) 388, 1022–1032

JMB

Available online at www.sciencedirect.com

ScienceDirect

ELSEVIER

E46K Parkinson's-Linked Mutation Enhances C-Terminal-to-N-Terminal Contacts in α-Synuclein

Carla C. Rospigliosi[1], Sebastian McClendon[1], Adrian W. Schmid[2], Trudy F. Ramlall[1], Patrick Barré[1], Hilal A. Lashuel[2] and David Eliezer[1]*

[1]*Department of Biochemistry and Program in Structural Biology, Weill Cornell Medical College, 1300 York Avenue, New York, NY 10065, USA*

[2]*Laboratory of Molecular Neurobiology and Neuroproteomics, Brain Mind Institute, Ecole Polytechnique Federale de Lausanne, CH-1015 Lausanne, Switzerland*

Received 2 February 2009; received in revised form 21 March 2009; accepted 28 March 2009
Available online 5 April 2009

Edited by S. Radford

Parkinson's disease (PD) is associated with the deposition of fibrillar aggregates of the protein α-synuclein (αS) in neurons. Intramolecular contacts between the acidic C-terminal tail of αS and its N-terminal region have been proposed to regulate αS aggregation, and two originally described PD mutations, A30P and A53T, reportedly reduce such contacts. We find that the most recently discovered PD-linked αS mutation E46K, which also accelerates the aggregation of the protein, does not interfere with C-terminal-to-N-terminal contacts and instead enhances such contacts. Furthermore, we do not observe a substantial reduction in such contacts in the two previously characterized mutants. Our results suggest that C-terminal-to-N-terminal contacts in αS are not strongly protective against aggregation, and that the dominant mechanism by which PD-linked mutations facilitate αS aggregation may be altering the physicochemical properties of the protein such as net charge (E46K) and secondary structure propensity (A30P and A53T).

Keywords: synuclein; Parkinson's; amyloid; protein aggregation; E46K

Introduction

α-Synuclein (αS) is a small 140-amino-acid protein that is intrinsically unstructured in aqueous solution and is enriched *in vivo* in the presynaptic terminals of the central nervous system.[1] Amyloid fibril aggregates of αS constitute a major component of characteristic proteinacious deposits formed in Parkinson's disease (PD) brains,[2,3] suggesting that αS aggregation may play a central role in the development of PD. Although the majority of PD cases appear to be sporadic, duplication or triplication of the αS gene[4,5] or the presence of any of three missense mutations A30P,[6] E46K,[7] and A53T[8] is associated with hereditary PD. The physiological functions of αS remain unclear, but various studies suggest roles of αS in modulating synaptic plasticity,[9] presynaptic vesicle pool size, and neurotransmitter release.[10–12]

Structurally, αS in its free state shows a weak propensity for helical structure throughout the N-terminal lipid-binding domain and a preference for more extended conformations in the acidic C-terminal tail region.[13] The PD-linked αS mutations A30P and A53T lead to a local decrease in the helical propensity of the protein—an effect that has been proposed to play a role in facilitating the aggregation of these two mutants into the β-sheet-rich amyloid fibril state.[14] The presence of amphipathic helical structure, combined with the known role of the hydrophobic NAC region of αS in mediating intermolecular interactions, also led to the hypothesis that transient long-range intramolecular contacts could protect αS from aggregation.[14] NMR paramagnetic relaxation enhancement (PRE) measurements confirmed the presence of long-range contacts in αS, but these were observed predominantly between the acidic C-terminal tail and both the NAC region and a region near the N-terminus of the protein.[15,16] A subsequent report indicated that the A30P and A53T mutations disrupt these long-range interactions, and this effect was proposed to underlie the ability of these mutants to facilitate αS aggregation *in vitro*.[17]

*Corresponding author. E-mail address: dae2005@med.cornell.edu.

Abbreviations used: PD, Parkinson's disease; αS, α-synuclein; PRE, paramagnetic relaxation enhancement; WT, wild type; RDC, residual dipolar coupling; HSQC, heteronuclear single quantum coherence; NIH, National Institutes of Health.

Here we report a detailed NMR structural study of the most recently discovered PD-linked αS mutation E46K. Previous work has shown that this mutant also increases the rate of αS aggregation *in vitro* and *in situ*,[18–20] suggesting that it also may result in the disruption of protective intramolecular long-range interactions. Surprisingly, we find that the E46K mutation does not decrease the interaction of the C-terminal tail of αS with either the NAC or the N-terminal regions of the protein and instead enhances these interactions. Furthermore, a comparison of all three PD-linked mutants with the wild-type (WT) protein indicates that none of the mutations abrogates these long-range contacts, suggesting that intramolecular contacts involving the C-terminal tail are unlikely to play a dominant role in regulating the aggregation rate of αS.

Results

Paramagnetic relaxation enhancement

PRE results from the dipolar interaction between the magnetic moments of a proton and an unpaired electron and is readily detectable up to distances of ~25 Å,[21,22] providing a sensitive tool for detecting long-range interactions in proteins. We measured PRE effects in E46K αS using spin labels conjugated to cysteine mutants S9C, E20C, S42C, H50C, A85C, E110C, P120C, and A140C in the E46K background. To allow a direct comparison with the WT protein, we augmented previously obtained data with data on S42C and H50C mutants with WT background. To provide a comparison with the two other PD-linked mutations A30P and A53T, we measured corresponding PRE data for both of these mutants.

Figure 1 shows a comparison of PRE effects between the WT and all three PD-linked mutants. As expected, spin-label positions near the N-terminus of the protein (S9 and E20) lead to significant broadening in the C-terminal tail of WT αS (Fig. 1a), and a spin label positioned in the C-terminal tail (P120) leads to broadening at the N-terminus. C-terminal labeling also leads to broadening in the NAC region of the protein, and labels in the NAC region (A85) lead to broadening in the C-terminal tail. These observations recapitulate previous studies[15,16,23] demonstrating contacts between the C-terminal tail of WT αS and the NAC and N-terminal regions. Interestingly, all spin-label positions within the lipid-binding domain of αS (residues ~1–100) led to a local broadening pattern that was significantly more extensive than that predicted based on a statistical model for an idealized Gaussian random-coil polypeptide. In addition, spin labels at previously unexamined positions (S42 and H50) indicated that this region of αS also interacts strongly with both the NAC region and the C-terminal tail of the protein.

Data for the E46K mutant (Fig. 1b) show the same features apparent for the WT, with spin labels at N-terminal positions 9 and 20 leading to significant broadening for residues 110–140 in the C-terminal tail, with labeling at position 85 leading to broadening for residues 100–120, and with a label at position 120 leading to broadening both at N-terminal residues 3–20 and at NAC region residues 75–95. Compared with the WT data, the long-range broadening effects appear to be somewhat more pronounced for the E46K mutant, and this is especially true for labels at the S42 and H50 positions.

Given that the E46K mutant was not observed to reduce long-range PRE compared to WT αS, we decided to examine the two remaining PD-linked mutants A30P (Fig. 1c) and A53T (Fig. 1d). Both mutants, like E46K, continue to exhibit broadening patterns similar to those observed for the WT protein. In particular, broadening effects associated with spin labeling at positions 20, 85, and 120, which most clearly illustrate interactions between the C-terminal tail and the N-terminal and NAC regions, are very similar to those observed for the WT protein.

Residual dipolar couplings

Residual dipolar couplings (RDCs) have become a useful tool in elucidating protein structures and dynamics, not only in proteins with a well-defined structure but also in disordered protein states.[24–27] Recent reports have suggested that RDCs in αS may reflect the presence of long-range contacts,[16,28] and that changes in the RDC profiles of PD-linked αS mutants reflect a decrease in such contacts.[17] We measured RDCs from E46K αS, as well as from the WT and A30P and A53T mutants, in order to compare all four variants. We also measured RDCs for a C-terminal fragment of αS (residues 103–140).

For bicelle-aligned WT αS, several distinct features are observed in the RDC data. Negative RDCs are observed for the N-terminal 10 residues, and positive but small RDCs are observed for residues 20–50. The remainder of the lipid-binding domain exhibits positive RDCs, with notable dips around positions 68 and 85. The C-terminal tail region exhibits two lobes of large positive RDCs separated by a dip around position 120, as previously reported.[16] Elimination of these C-terminal lobes in the presence of the PD-linked mutations A30P and A53T, as well as in the presence of polycations or protein denaturants, led to the conclusion that this

Fig. 1. PRE data for (a) αS WT, (b) αS E46K, (c) αS A30P, and (d) αS A53T. Histograms show the intensity ratio for those peaks that are well-resolved in ^{1}H–^{15}N HSQC spectra. Red curves represent the broadening expected from a theoretical random-coil model. Green curves represent a seven-residue moving average of the data from the WT protein and are provided to facilitate a comparison of mutant and WT data. Some data for the WT protein have been reported previously[23] and are included for purposes of comparison.

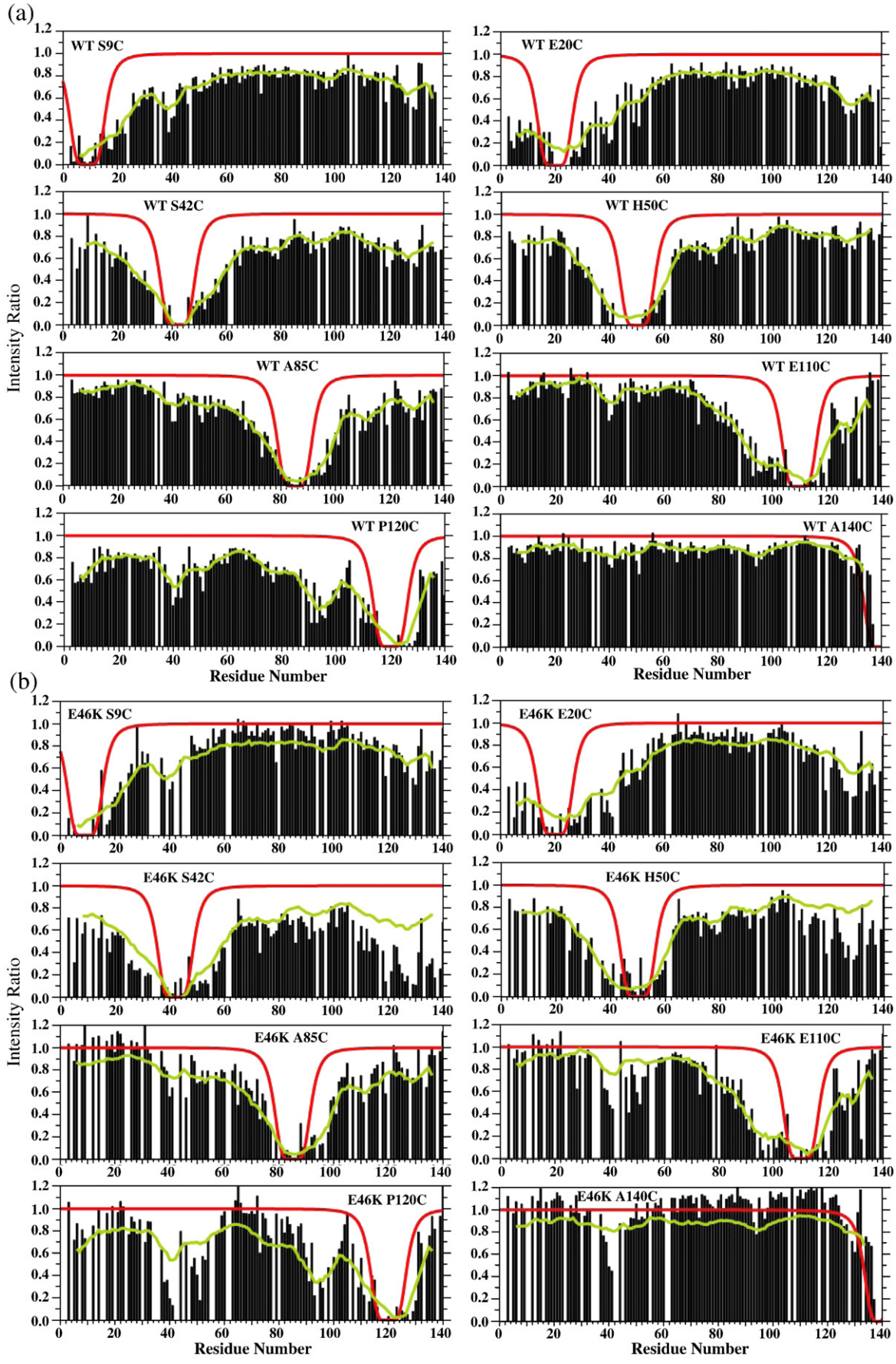

Fig. 1 *(legend on previous page)*

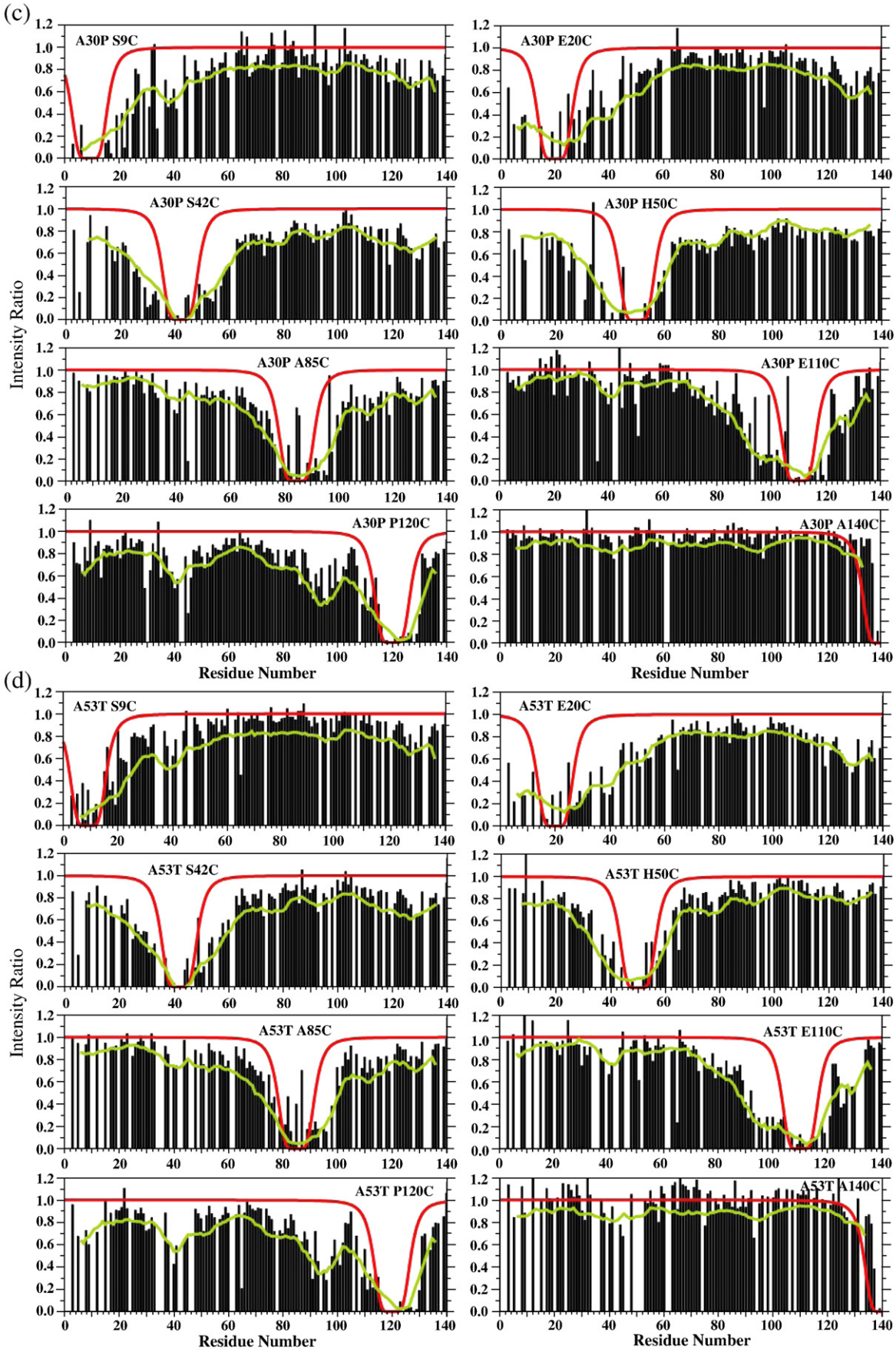

Fig. 1 *(legend on page 1023)*

feature arises as a result of long-range contacts in the WT protein that are eliminated in the presence of PD-linked mutations.[16,17]

Surprisingly, RDC data for the bicelle-aligned E46K mutant appeared highly similar to those obtained for the WT protein. In particular, the double-lobed feature in the C-terminal tail of the protein was completely preserved. Given this unexpected result, we proceeded to examine the remaining two PD-linked mutations, A30P and A53T. In both cases, we obtained RDC data that were highly similar to both WT and E46K data, and again the double-lobed feature in the C-terminal tail of the protein was preserved.

To further investigate whether the double-lobed feature in the C-terminal tail of αS might result from long-range interactions, we prepared a fragment of the protein consisting of residues 103–140 and measured RDCs from this fragment aligned in a bicelle medium. The data (Fig. 2a) reveal that the RDC values for the isolated C-terminal tail fragment overlay the data for the corresponding residues in the intact full-length protein quite well, demonstrating that the remainder of the protein is not involved in determining the pattern of RDC values in the C-terminal tail of αS.

Residual secondary structure

To assess the influence of the E46K mutation on residual secondary structure in αS, we calculated the deviations of the observed C^{α} chemical shifts from values expected for peptides without secondary structure preferences (so-called secondary C^{α} shifts). Positive deviations are expected for regions preferring helical regions of ϕ,ψ space, while negative values are indicative of a preference for extended structures. The data indicate that there are few differences between the secondary shifts observed for the E46K mutant and those previously reported for the WT protein.[13] Immediately adjacent to the site of the mutation, a few residues exhibit a change from negative secondary shifts to positive values, indicating a slight increase in local helix propensity.

Discussion

αS forms amyloid fibrils found in Lewy bodies, a hallmark of the neurodegenerative disorder PD.[29] The formation of fibrils is thought to be a stepwise process in which αS goes through conformational changes, followed by oligomerization and, finally, assembly into mature fibrils.[30] Conformational transitions that modulate initial aggregation steps leading to oligomer formation are likely to be particularly crucial because the clearest common effect of all three PD-linked αS mutations is to increase the protein's oligomerization rate,[7,31] suggesting that oligomeric states may be the toxic species involved in the pathogenesis of PD. Although it seems likely that the PD-linked αS mutations influence the aggregation

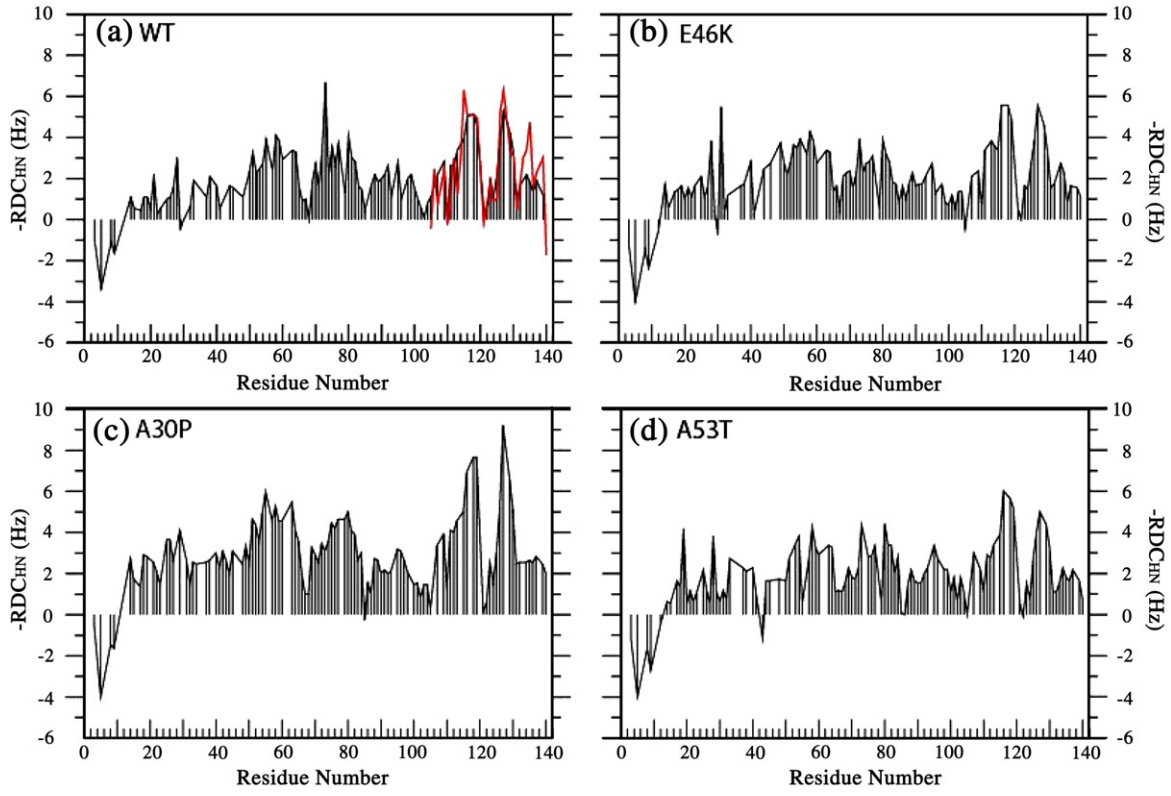

Fig. 2. RDCs for (a) αS WT, (b) αS E46K, (c) αS A30P, and (d) αS A53T in bicelles. RDCs for the C-terminal tail of αS (residues 103–140) in bicelles are overlaid on the corresponding plot for αS WT (a) in red. Note that the RDC sign is inverted according to convention.

rate of the protein by altering its physicochemical and/or structural properties, a precise understanding of their effects remains elusive.

Previous structural models of how PD mutations influence αS aggregation

αS has been categorized as a natively unfolded or intrinsically unstructured protein in aqueous solution.[32] Initial analysis of the conformational preferences of the WT protein indicated that αS has a weak preference for a helical structure distributed throughout the N-terminal lipid-binding domain of the protein, while the C-terminal tail has a preference for a more extended structure.[13] Similar studies performed on A30P and A53T showed that those two mutations lead to a local decrease in helical preference, leading to one model in which the mutations enhance the conversion of αS into the β-sheet-rich fibrillar conformation by destabilizing the natural preference of the protein for its native helical structure, which is fully materialized in the lipid-bound state.[14] An alternative model proposed that amphipathic helical motifs could interact intramolecularly with the hydrophobic NAC region of the protein and thereby decrease intermolecular hydrophobic interactions that lead to αS aggregation. In this model, disruption of amphipathic helix formation by PD-linked mutations would decrease protective intramolecular interactions and thereby accelerate αS aggregation.[14] Subsequent data showed that long-range intramolecular interactions do, in fact, exist in αS but involve the acidic C-terminal tail of the protein, which interacts with the N-terminal and NAC regions.[15,16] It was further reported that the two known (at that time) PD-linked mutations A30P and A53T perturbed long-range contacts involving the C-terminal tail in WT αS,[17] leading to broad acceptance of the idea that perturbation of such contacts may be an important mechanism by which mutations increase the aggregation propensity of αS.

E46K mutation enhances long-range interactions in αS

To investigate the potential effects of the most recently discovered PD-linked αS mutation E46K on long-range contacts within αS, we first evaluated such contacts by examining PRE effects, which reflect a spatial proximity of ~25 Å or less between a given residue and the location of a covalently attached spin label. This method was originally used to document long-range contacts in WT αS.[15,16] According to the PRE data, there is no decrease in long-range contacts in the E46K mutant relative to that in the WT protein (Fig. 1a and b). Instead, the data suggest an increased interaction between the C-terminal tail and the NAC and N-terminal regions, as well as previously unnoted interactions between the region around residues 40–50 and both the C-terminal and the NAC regions of the protein. Notably, these results are in agreement with the previous observation that E46K αS elutes slightly later than the WT protein during size-exclusion chromatography, suggesting that it is somewhat more compact.[33]

We further examined PRE data from the A30P and A53T PD-linked αS mutants for indications that they perturb long-range interactions (Fig. 1c and d). Data for both mutants closely resemble those for the WT protein. Thus, as monitored by PRE data, long-range interactions persist in both E46K and the two other PD-linked αS mutations. Previously, it was reported that the A30P and A53T mutations led to a slight decrease in long-range PRE effects in αS.[17] However, the reported decrease was likely within the range of experimental error, and the extent of the reduction was minor, leading to the same conclusion drawn from our own data, namely, that long-range contacts, as monitored by PRE data, persist for both PD-linked mutants. A recent study of transglutaminase-induced αS cross-linking also suggests that long-range contacts in WT αS are not perturbed by the A30P and A53T mutations.[34]

Indeed, rather than PRE data, changes in RDCs in the C-terminal region of αS in the presence of the A30P and A53T mutations were the primary basis for concluding that these mutations perturb long-range interactions within the protein.[17] Therefore, we examined the effects of the E46K mutation on αS RDC data (Fig. 2). Surprisingly, we found that the E46K mutation does not substantially alter the pattern of RDC values observed in the C-terminal tail of αS or, for that matter, in the remainder of the protein. Thus, RDCs do not indicate any reduction in long-range structure between E46K and WT αS. Because of this unexpected result, we decided to obtain RDC data for the A30P and A53T mutants, as well, for purposes of comparison. We were again surprised to observe that the pattern of RDCs in the C-terminal tail, as well as in the rest of the protein, closely resembles that of the WT protein for both of these mutants, providing no indication for changes in long-range structure.

RDCs in the C-terminal tail of αS do not originate from long-range interactions

Recently, we reported structural studies of the two other human synuclein family members β-synuclein and γ-synuclein.[23] These studies showed that these proteins largely lack the long-range contacts present in αS based on PRE data, yet do show, like αS, large RDC values in their C-terminal tails. Based on these observations, we suggested[23,35] that the RDCs in the C-terminal tail of αS may not be a result of long-range interactions within the protein, as had been previously concluded.[28] Instead, we observed a qualitative correlation between the RDCs and α-carbon secondary shifts, suggesting that the RDC patterns may arise as a result of local secondary structure preference, as has been noted previously.[26] Here, we fail to observe changes to RDCs in the C-terminal tail of αS in the presence of any of the three PD-linked mutations, suggesting either that the

mutations do not perturb a long-range structure or that the RDCs do not reflect a long-range structure, or both. To further test whether RDCs in the C-terminal tail of αS arise from long-range interactions, we generated a C-terminal fragment of the protein and recorded RDCs for this isolated fragment. The results (Fig. 2a) clearly show that the pattern of RDCs in the C-terminal tail of the intact protein is closely preserved in the isolated C-terminal fragment, indicating that the observed RDCs do not result from long-range intramolecular interactions.

Role of the acidic C-terminal tail in αS aggregation

A model in which long-range intramolecular contacts within αS are protective is appealing because it has a direct analogy in well-structured proteins, which bury hydrophobic cores through a long-range tertiary structure and thereby avoid nonspecific protein–protein interactions and aggregation. In turn, the perturbation of such interactions by mutations in αS could facilitate aggregation in a manner analogous to destabilizing mutations in native proteins, causing exposure of hydrophobic patches leading to aggregation. The data we present here, however, suggest that the mechanism by which PD-linked mutations facilitate αS aggregation does not primarily involve the release of contacts between the C-terminal tail and the N-terminal regions of the protein. Indeed, for the A30P and A53T mutations, these contacts appear essentially unperturbed; for the more recently identified E46K mutation, these contacts appear to be enhanced. Additional evidence arguing against a protective role for C-terminal-to-N-terminal contacts in αS is provided by a recent study of αS phosphorylation at Ser129.[36] Phosphorylation at this site is shown to release the C-terminus from its interactions with N-terminal regions, yet, at the same time, to significantly inhibit αS aggregation.

That the C-terminal tail plays any role at all in αS aggregation is firmly established by data demonstrating that C-terminally truncated forms of αS aggregate more readily than the WT protein.[37–39] Thus, the C-terminus appears to play a protective role, but how is this role effected? The most remarkable property of the C-terminal tail of αS is its acidic nature. It contains 14 negatively charged side chains and no positive charges past position 102. Such a highly charged polypeptide segment can be expected to lead to significant electrostatic self-repulsion and to greatly increase the solubility of any attached protein sequence. Thus, electrostatics alone may be sufficient to explain the protective effects of the αS C-terminal tail and why its truncation greatly increases αS aggregation.[1] Under this model, increasing the negative charge of the C-terminal tail through phosphorylation at Ser129 would clearly be expected to increase solubility and to decrease aggregation, as observed.[36]

Simple electrostatics can also readily explain the long-range interactions of the C-terminal tail of αS with the remainder of the protein (i.e., the N-terminal domain). The N-terminal lipid-binding domain of αS contains many basic residues (a net charge of +6 at neutral pH), which are necessary for the interaction of the protein with negatively charged phospholipids.[40] Thus, it is not surprising that the oppositely charged N-terminal and C-terminal regions of the protein would form intramolecular interactions. Such interactions could effectively neutralize some of the negative charges of the C-terminal tail, but a net charge of −9 remains, leading to significant intermolecular electrostatic repulsion. Truncation of the C-terminal tail leaves a lesser net charge of +5, with accordingly reduced repulsion and increased aggregation. Addition of polycations[41] or metal ions[42] can also neutralize the negative charge of the C-terminal tail, leading to its release from long-range interactions. However, enhanced aggregation in the presence of polycations or metal ions likely results from the reduction in the net effective charge of the protein,[43,44] rather than from the release of the C-terminal tail. Similarly, a recent study demonstrates that high salt concentrations also decrease C-terminal-to-N-terminal contacts in αS, indicating a significant electrostatic component.[45] Again, however, increased aggregation of αS at high ionic strength[46] can primarily be attributed to the reduction in intermolecular electrostatic repulsion by the same charge screening effect that leads to the observed incidental decrease in C-terminal-to-N-terminal contacts. Our current data provide further corroboration. The E46K mutation of αS increases the positive charge of the N-terminal lipid-binding domain, which would be expected to enhance interactions with the negatively charged C-terminal domain, as we indeed observed. Furthermore, the most clearly increased interactions involved locations near the site of the mutation (as indicated by greatly increased PRE effects with labels at positions 42 and 50). In contrast, the two other PD-linked mutations A30P and A53T do not alter the charge of the lipid-binding domain of the protein and, in turn, do not appear to influence its interactions with the C-terminal tail.

Mechanism by which PD-linked mutations influence αS aggregation

Since PD-linked mutations do not substantially reduce long-range contacts involving the C-terminal tail of αS, how do they enhance αS aggregation? Despite the appeal of our original model invoking effects on long-range contacts, the alternative model in which local changes in the physicochemical properties of the polypeptide dominate appears, at present, to be most consistent with the available data. Firstly, both A30P and A53T mutations have been shown experimentally to reduce local helical propensity, as would be expected based on the natural secondary structure propensities of alanine, threonine, and proline. Unlike the first two mutations, the E46K mutation increases, albeit slightly, the local helix propensity of the protein (Fig. 3),

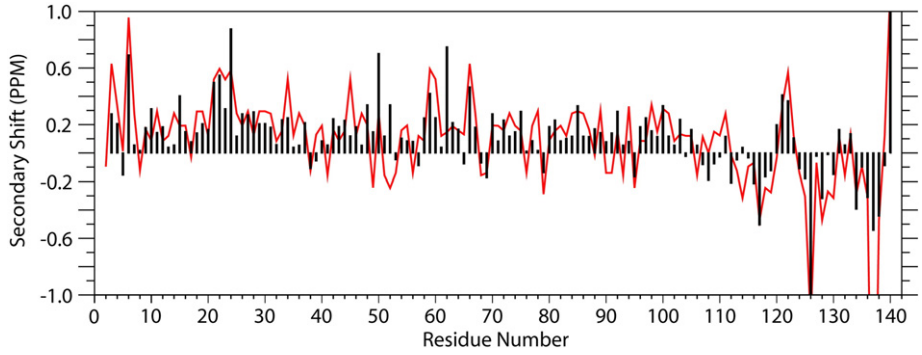

Fig. 3. C^{α} secondary shifts for αS E46K in the free state as a function of residue number (black bars) overlaid with the C^{α} values previously reported for WT αS (red line).[13] Positive values indicate a propensity for helical structure, while negative values indicate a preference for strand-like structure.

which, under this model, should lead to decreased aggregation, but this mutation also decreases the net charge of the protein by 2, an effect that could be expected to counteract and apparently dominate a local increase in helicity. Another example consistent with this argument is the case of mouse αS. The mouse protein aggregates more readily than WT αS, and recent NMR studies have indicated that this variant exhibits reduced C-terminal-to-N-terminal contacts.[47] The reduced contacts may be ascribed to the elimination of one negative charge (D121) in the C-terminal tail of mouse αS. The increased aggregation rate, however, rather than being associated with the partial release of the C-terminal tail, likely results from the reduction in the net charge of the protein, as well as from two further sequence changes (A53T and S87N), which would engender an increased local preference for β-strand structure. Further support for the importance of changes in physicochemical properties in protein aggregation is provided by recent work showing that changes in secondary structure propensity, charge, and hydrophobicity can quantitatively account for the effects of mutations on the fibrillization rates of many amyloid-forming proteins.[48] Indeed, a recent study employed just such an algorithm to successfully predict the expected aggregation rates of β-synuclein, a close homologue of αS, as well as a number of αS variants that incorporate β-synuclein sequence changes.[49] Since this algorithm succeeds by relying purely on the physicochemical properties of the individual amino acid sequences and does not include any consideration of long-range contacts with the C-terminal tail, it can be concluded that the former plays the dominant role in determining the aggregation rate of αS.

Conclusions

A current paradigm showing how αS aggregation is enhanced in PD invokes a protective role for long-range interactions between the C-terminal domain and the N-terminal domain of the protein, which are perturbed by PD-linked mutations or by external factors such as polycation binding. Our results indicate that the E46K PD-linked αS mutation, despite enhancing αS aggregation, does not perturb C-terminal-to-N-terminal contacts in the protein and instead enhances such contacts. In light of this counterexample, this paradigm cannot be considered general. Furthermore, closer examination indicates that other PD-linked αS mutations do not substantially reduce C-terminal-to-N-terminal contacts either. In place of the existing paradigm, we suggest an alternative model in which the C-terminal tail inhibits αS aggregation primarily because of the net negative charge that it lends to the intact protein. The C-terminal tail does indeed interact with the oppositely charged N-terminal lipid-binding domain, but these interactions do not exert a dominant regulatory effect on αS aggregation. Instead, any reduction in the net charge of the protein, either through truncation of the C-terminal tail or through sequence changes associated with disease (e.g., E46K in PD) or with divergent evolution (e.g., D121G in mouse αS), leads to enhanced aggregation. Mutations that do not alter net charge can apparently influence aggregation by altering the secondary structure preferences of the polypeptide chain (e.g., A30P and A53T in PD) or possibly by altering the hydrophobicity of the protein as well. This model is consistent with recent studies highlighting the importance of the physicochemical properties of protein sequences in determining their propensity to form amyloid aggregates.

Materials and Methods

Protein expression and purification

αS mutants were generated using site-directed mutagenesis of the WT plasmid construct (kindly provided by Dr. Peter Lansbury, Harvard Medical School) and expressed in *Escherichia coli* BL21(DE3) cells. Recombinant proteins were uniformly labeled by growing cells in M9 minimal media supplemented with [^{13}C]glucose and/or [^{15}N]ammonium chloride at 37 °C to an OD_{600} of ~0.6,

followed by induction with 1 mM IPTG. Cells were harvested 4 h after induction, followed by purification of the protein using previously reported protocols.[13]

Preparation of αS C-terminal fragment

WT αS was dissolved in 50 mM Tris and 150 mM NaCl (pH 7.6) and subjected to limited proteolysis using an αS/trypsin (Promega) mass ratio of 100:1 at 37 °C for 24 h.[34] Reactions were quenched by lowering the sample's pH to ~3.0 using trifluoroacetic acid and stored at −20 °C. Defrosted samples were restored to neutral pH, and the resulting fragments, including the intact C-terminal tail (residues 103–140), were separated using size-exclusion chromatography (Superdex 75HR 10/30 column; GE Healthcare) in 50 mM ammonium bicarbonate (pH 7.5), followed by anion-exchange chromatography. Final fractions were pooled, desalted, and lyophilized for storage.

NMR spectroscopy

Free-state samples were prepared by directly dissolving lyophilized protein in 100 mM NaCl and 10 mM Na_2HPO_4 (pH 7.4; phosphate-buffered saline) in 90%/10% H_2O/D_2O, followed by removal of any large-scale aggregate using Microcon YM-100 centrifugal filters (Millipore). NMR experiments were performed on either a 600-MHz Varian INOVA spectrometer (Weill Cornell Medical College) or 800- or 900-MHz Bruker AVANCE spectrometers (New York Structural Biology Center) at a sample temperature of 10 °C. Resonance assignments for αS E46K in the free state were based on HNCACB/CBCACONH and HNCACO/HNCO triple-resonance experiments. All NMR data were processed with NMRPipe[50] and analyzed using NMRView.[51] Spectra were referenced indirectly to 2,2-dimethyl-2-silapentane-5-sulfonate and ammonia[52] using the known chemical shift of water. Random-coil values obtained from linear hexapeptides in 1 M urea (pH 5.0) and 25 °C[53] were used to calculate C^{α} secondary shifts.

RDC measurements were made using two-dimensional IPAP experiments based on heteronuclear single quantum coherence (HSQC).[54] Samples were aligned using bicelles[55] prepared with 7.4% (wt/vol) pentaethylene glycol monooctyl ether (C_8E_5)/octanol (Sigma) at a protein concentration of 140 μM. Alignment was verified by measuring the deuterium quadrupolar splitting of the water line.

PRE effects were measured using cysteine mutants created through site-directed mutagenesis against WT, A30P, E46K, and A53T backgrounds. Cysteines were introduced at positions 9, 20, 42, 50, 85, 110, 120, and 140 in the protein sequence. The spin-label reagent 1-oxy-2,2,5,5-tetramethyl-D-pyrroline-3-methyl-methanethiosulfonate (Toronto Research Chemicals) was added at a 10-fold molar excess to protein-containing solutions, and excess spin label was removed after a 2-h incubation at room temperature by passing samples three times through buffer-equilibrated spin columns packed with Sephadex G-25 fine matrix (GE Healthcare). Control samples were prepared by adding DTT to the 1-oxy-2,2,5,5-tetramethyl-D-pyrroline-3-methyl-methanethiosulfonate-labeled proteins to reduce the nitroxide spin label from the protein. This approach was used instead of directly reducing the nitroxide spin label or using a nonparamagnetic analogue in order to control for the possibility of noncovalent and nonspecific binding of the spin label to aromatic or other protein residues. PRE effects were obtained as normalized peak heights from the HSQC spectra of matched spin-labeled and control samples collected at 10 °C using a protein concentration of 70 μM. Theoretical PRE curves were calculated as previously described.[23]

Acknowledgements

This work was supported by National Institutes of Health (NIH) grants AG019391 and AG025440, the Irma T. Hirschl Foundation, and a gift from Herbert and Ann Siegel (to D.E.) and NIH grant NS058137 (to S.M.). We thank Dr. Peter Lansbury (Harvard Medical School) for the kind gift of expression vectors, and Mike Goger, Kaushik Dutta, and Shibani Bhattacharya (New York Structural Biology Center) for support with NMR data collection and processing. D.E. is a member of the New York Structural Biology Center, which is a STAR center supported by the New York State Office of Science, Technology, and Academic Research, was supported by NIH grant P41 GM66354 and received funds from the NIH (USA), the Keck Foundation, the New York State, and the NYC Economic Development Corporation for the purchase of 900-MHz spectrometers.

References

1. Eliezer, D. (2008). Protein folding and aggregation in *in vitro* models of Parkinson's disease: structure and function of α-synuclein. In *Parkinson's Disease: Molecular and Therapeutic Insights from Model Systems* (Nass, R. & Prezedborski, S., eds), pp. 575–595, Academic Press, New York.
2. Spillantini, M. G., Schmidt, M. L., Lee, V. M., Trojanowski, J. Q., Jakes, R. & Goedert, M. (1997). Alpha-synuclein in Lewy bodies. *Nature*, **388**, 839–840.
3. Lee, V. M. & Trojanowski, J. Q. (2006). Mechanisms of Parkinson's disease linked to pathological alpha-synuclein: new targets for drug discovery. *Neuron*, **52**, 33–38.
4. Singleton, A. B., Farrer, M., Johnson, J., Singleton, A., Hague, S., Kachergus, J. *et al.* (2003). Alpha-synuclein locus triplication causes Parkinson's disease. *Science*, **302**, 841.
5. Chartier-Harlin, M. C., Kachergus, J., Roumier, C., Mouroux, V., Douay, X., Lincoln, S. *et al.* (2004). Alpha-synuclein locus duplication as a cause of familial Parkinson's disease. *Lancet*, **364**, 1167–1169.
6. Kruger, R., Kuhn, W., Muller, T., Woitalla, D., Graeber, M., Kosel, S. *et al.* (1998). Ala30Pro mutation in the gene encoding alpha-synuclein in Parkinson's disease. *Nat. Genet.* **18**, 106–108.
7. Zarranz, J. J., Alegre, J., Gomez-Esteban, J. C., Lezcano, E., Ros, R., Ampuero, I. *et al.* (2004). The new mutation, E46K, of alpha-synuclein causes Parkinson and Lewy body dementia. *Ann. Neurol.* **55**, 164–173.
8. Polymeropoulos, M. H., Lavedan, C., Leroy, E., Ide, S. E., Dehejia, A., Dutra, A. *et al.* (1997). Mutation in the alpha-synuclein gene identified in families with Parkinson's disease. *Science*, **276**, 2045–2047.
9. George, J. M., Jin, H., Woods, W. S. & Clayton, D. F. (1995). Characterization of a novel protein regulated

during the critical period for song learning in the zebra finch. *Neuron*, **15**, 361–372.
10. Abeliovich, A., Schmitz, Y., Farinas, I., Choi-Lundberg, D., Ho, W. H., Castillo, P. E. *et al.* (2000). Mice lacking alpha-synuclein display functional deficits in the nigrostriatal dopamine system. *Neuron*, **25**, 239–252.
11. Murphy, D. D., Rueter, S. M., Trojanowski, J. Q. & Lee, V. M. (2000). Synucleins are developmentally expressed, and alpha-synuclein regulates the size of the presynaptic vesicular pool in primary hippocampal neurons. *J. Neurosci.* **20**, 3214–3220.
12. Cabin, D. E., Shimazu, K., Murphy, D., Cole, N. B., Gottschalk, W., McIlwain, K. L. *et al.* (2002). Synaptic vesicle depletion correlates with attenuated synaptic responses to prolonged repetitive stimulation in mice lacking alpha-synuclein. *J. Neurosci.* **22**, 8797–8807.
13. Eliezer, D., Kutluay, E., Bussell, R., Jr & Browne, G. (2001). Conformational properties of alpha-synuclein in its free and lipid-associated states. *J. Mol. Biol.* **307**, 1061–1073.
14. Bussell, R., Jr & Eliezer, D. (2001). Residual structure and dynamics in Parkinson's disease-associated mutants of alpha-synuclein. *J. Biol. Chem.* **276**, 45996–46003.
15. Dedmon, M. M., Christodoulou, J., Wilson, M. R. & Dobson, C. M. (2005). Heat shock protein 70 inhibits alpha-synuclein fibril formation via preferential binding to prefibrillar species. *J. Biol. Chem.* **280**, 14733–14740.
16. Bertoncini, C. W., Jung, Y. S., Fernandez, C. O., Hoyer, W., Griesinger, C., Jovin, T. M. & Zweckstetter, M. (2005). Release of long-range tertiary interactions potentiates aggregation of natively unstructured alpha-synuclein. *Proc. Natl Acad. Sci. USA*, **102**, 1430–1435.
17. Bertoncini, C. W., Fernandez, C. O., Griesinger, C., Jovin, T. M. & Zweckstetter, M. (2005). Familial mutants of alpha-synuclein with increased neurotoxicity have a destabilized conformation. *J. Biol. Chem.* **280**, 30649–30652.
18. Choi, W., Zibaee, S., Jakes, R., Serpell, L. C., Davletov, B., Crowther, R. A. & Goedert, M. (2004). Mutation E46K increases phospholipid binding and assembly into filaments of human alpha-synuclein. *FEBS Lett.* **576**, 363–368.
19. Greenbaum, E. A., Graves, C. L., Mishizen-Eberz, A. J., Lupoli, M. A., Lynch, D. R., Englander, S. W. *et al.* (2005). The E46K mutation in alpha-synuclein increases amyloid fibril formation. *J. Biol. Chem.* **280**, 7800–7807.
20. Pandey, N., Schmidt, R. E. & Galvin, J. E. (2006). The alpha-synuclein mutation E46K promotes aggregation in cultured cells. *Exp. Neurol.* **197**, 515–520.
21. Gillespie, J. R. & Shortle, D. (1997). Characterization of long-range structure in the denatured state of staphylococcal nuclease. I. Paramagnetic relaxation enhancement by nitroxide spin labels. *J. Mol. Biol.* **268**, 158–169.
22. Gillespie, J. R. & Shortle, D. (1997). Characterization of long-range structure in the denatured state of staphylococcal nuclease: II. Distance restraints from paramagnetic relaxation and calculation of an ensemble of structures. *J. Mol. Biol.* **268**, 170–184.
23. Sung, Y. H. & Eliezer, D. (2007). Residual structure, backbone dynamics, and interactions within the synuclein family. *J. Mol. Biol.* **372**, 689–707.
24. Tjandra, N. & Bax, A. (1997). Direct measurement of distances and angles in biomolecules by NMR in a dilute liquid crystalline medium. *Science*, **278**, 1111–1114.
25. Shortle, D. & Ackerman, M. S. (2001). Persistence of native-like topology in a denatured protein in 8 M urea. *Science*, **293**, 487–489.
26. Mohana-Borges, R., Goto, N. K., Kroon, G. J., Dyson, H. J. & Wright, P. E. (2004). Structural characterization of unfolded states of apomyoglobin using residual dipolar couplings. *J. Mol. Biol.* **340**, 1131–1142.
27. Eliezer, D. (2007). Characterizing residual structure in disordered protein states using nuclear magnetic resonance. *Methods Mol. Biol.* **350**, 49–67.
28. Bernado, P., Bertoncini, C. W., Griesinger, C., Zweckstetter, M. & Blackledge, M. (2005). Defining long-range order and local disorder in native alpha-synuclein using residual dipolar couplings. *J. Am. Chem. Soc.* **127**, 17968–17969.
29. Spillantini, M. G., Crowther, R. A., Jakes, R., Hasegawa, M. & Goedert, M. (1998). Alpha-synuclein in filamentous inclusions of Lewy bodies from Parkinson's disease and dementia with Lewy bodies. *Proc. Natl Acad. Sci. USA*, **95**, 6469–6473.
30. Caughey, B. & Lansbury, P. T. (2003). Protofibrils, pores, fibrils, and neurodegeneration: separating the responsible protein aggregates from the innocent bystanders. *Annu. Rev. Neurosci.* **26**, 267–298.
31. Conway, K. A., Lee, S. J., Rochet, J. C., Ding, T. T., Williamson, R. E. & Lansbury, P. T., Jr (2000). Acceleration of oligomerization, not fibrillization, is a shared property of both alpha-synuclein mutations linked to early-onset Parkinson's disease: implications for pathogenesis and therapy. *Proc. Natl Acad. Sci. USA*, **97**, 571–576.
32. Weinreb, P. H., Zhen, W., Poon, A. W., Conway, K. A. & Lansbury, P. T., Jr (1996). NACP, a protein implicated in Alzheimer's disease and learning, is natively unfolded. *Biochemistry*, **35**, 13709–13715.
33. Fredenburg, R. A., Rospigliosi, C., Meray, R. K., Kessler, J. C., Lashuel, H. A., Eliezer, D. & Lansbury, P. T., Jr (2007). The impact of the E46K mutation on the properties of alpha-synuclein in its monomeric and oligomeric states. *Biochemistry*, **46**, 7107–7118.
34. Schmid, A. W., Chiappe, D., Pignat, V., Grimminger, V., Hang, I., Moniatte, M. & Lashuel, H. A. (2009). Dissecting the mechanisms of tissue transglutaminase-induced cross-linking of alpha-synuclein: implications for the pathogenesis of Parkinson's disease. *J. Biol. Chem.* In press. doi:10.1074/jbc.M809067200.
35. Eliezer, D. (2009). Biophysical characterization of intrinsically disordered proteins. *Curr. Opin. Struct. Biol.* **19**, 23–30.
36. Paleologou, K. E., Schmid, A. W., Rospigliosi, C. C., Kim, H. Y., Lamberto, G. R., Fredenburg, R. A. *et al.* (2008). Phosphorylation at Ser-129 but not the phosphomimics S129E/D inhibits the fibrillation of alpha-synuclein. *J. Biol. Chem.* **283**, 16895–16905.
37. Crowther, R. A., Jakes, R., Spillantini, M. G. & Goedert, M. (1998). Synthetic filaments assembled from C-terminally truncated alpha-synuclein. *FEBS Lett.* **436**, 309–312.
38. Serpell, L. C., Berriman, J., Jakes, R., Goedert, M. & Crowther, R. A. (2000). Fiber diffraction of synthetic alpha-synuclein filaments shows amyloid-like cross-beta conformation. *Proc. Natl Acad. Sci. USA*, **97**, 4897–4902.
39. Murray, I. V., Giasson, B. I., Quinn, S. M., Koppaka, V., Axelsen, P. H., Ischiropoulos, H. *et al.* (2003). Role of alpha-synuclein carboxy-terminus on fibril formation *in vitro*. *Biochemistry*, **42**, 8530–8540.
40. Bussell, R., Jr & Eliezer, D. (2003). A structural and functional role for 11-mer repeats in alpha-synuclein

and other exchangeable lipid binding proteins. *J. Mol. Biol.* **329**, 763–778.
41. Fernandez, C. O., Hoyer, W., Zweckstetter, M., Jares-Erijman, E. A., Subramaniam, V., Griesinger, C. & Jovin, T. M. (2004). NMR of alpha-synuclein–polyamine complexes elucidates the mechanism and kinetics of induced aggregation. *EMBO J.* **23**, 2039–2046.
42. Sung, Y. H., Rospigliosi, C. & Eliezer, D. (2006). NMR mapping of copper binding sites in alpha-synuclein. *Biochim. Biophys. Acta*, **1764**, 5–12.
43. Goers, J., Uversky, V. N. & Fink, A. L. (2003). Polycation-induced oligomerization and accelerated fibrillation of human alpha-synuclein *in vitro*. *Protein Sci.* **12**, 702–707.
44. Uversky, V. N., Li, J. & Fink, A. L. (2001). Metal-triggered structural transformations, aggregation, and fibrillation of human alpha-synuclein. A possible molecular link between Parkinson's disease and heavy metal exposure. *J. Biol. Chem.* **276**, 44284–44296.
45. Kim, H. Y., Cho, M. K., Riedel, D., Fernandez, C. O. & Zweckstetter, M. (2008). Dissociation of amyloid fibrils of alpha-synuclein in supercooled water. *Angew Chem. Int. Ed. Engl.* **47**, 5046–5048.
46. Munishkina, L. A., Henriques, J., Uversky, V. N. & Fink, A. L. (2004). Role of protein–water interactions and electrostatics in alpha-synuclein fibril formation. *Biochemistry*, **43**, 3289–3300.
47. Wu, K. P., Kim, S., Fela, D. A. & Baum, J. (2008). Characterization of conformational and dynamic properties of natively unfolded human and mouse alpha-synuclein ensembles by NMR: implication for aggregation. *J. Mol. Biol.* **378**, 1104–1115.
48. Chiti, F., Stefani, M., Taddei, N., Ramponi, G. & Dobson, C. M. (2003). Rationalization of the effects of mutations on peptide and protein aggregation rates. *Nature*, **424**, 805–808.
49. Rivers, R. C., Kumita, J. R., Tartaglia, G. G., Dedmon, M. M., Pawar, A., Vendruscolo, M. *et al.* (2008). Molecular determinants of the aggregation behavior of alpha- and beta-synuclein. *Protein Sci.* **17**, 887–898.
50. Delaglio, F., Grzesiek, S., Vuister, G. W., Zhu, G., Pfeifer, J. & Bax, A. (1995). NMRPipe: a multidimensional spectral processing system based on UNIX pipes [see comments]. *J. Biomol. NMR*, **6**, 277–293.
51. Johnson, B. A. & Blevins, R. A. (1994). NMRView: a computer program for the visualization and analysis of NMR data. *J. Biomol. NMR*, **4**, 603–614.
52. Wishart, D. S., Bigam, C. G., Yao, J., Abildgaard, F., Dyson, H. J., Oldfield, E. *et al.* (1995). ^{1}H, ^{13}C and ^{15}N chemical shift referencing in biomolecular NMR. *J. Biomol. NMR*, **6**, 135–140.
53. Wishart, D. S., Bigam, C. G., Holm, A., Hodges, R. S. & Sykes, B. D. (1995). ^{1}H, ^{13}C and ^{15}N random coil NMR chemical shifts of the common amino acids: I. Investigations of nearest-neighbor effects. *J. Biomol. NMR*, **5**, 67–81.
54. Ottiger, M., Delaglio, F. & Bax, A. (1998). Measurement of *J* and dipolar couplings from simplified two-dimensional NMR spectra. *J. Magn. Reson.* **131**, 373–378.
55. Otting, G., Ruckert, M., Levitt, M. H. & Moshref, A. (2000). NMR experiments for the sign determination of homonuclear scalar and residual dipolar couplings. *J. Biomol. NMR*, **16**, 343–346.